Curie temperatures of annealed FePt nanoparticle systems

Chuan-Bing Rong, Yang Li, and J. Ping Liu[a)]
Department of Physics, University of Texas at Arlington, Arlington, Texas 76019

(Presented on 8 January 2007; received 26 October 2006; accepted 21 November 2006; published online 28 March 2007)

The chemically synthesized Fe_xPt_{100-x} nanoparticles with controlled compositions were annealed to transfer the disordered face-centered-cubic structure to the ordered structure. It was found that the $L1_0$ FePt structure can be formed in the wide compositional region of $x=40-68$, and lower or higher Fe content leads to formation of the $L1_2$ $FePt_3$ or Fe_3Pt phase, respectively. The Néel temperature of $L1_2$ $FePt_3$ phase and Curie temperatures (T_C) of $L1_0$ FePt and $L1_2$ Fe_3Pt phases are all strongly composition dependent. The room-temperature saturation magnetization has an abnormal dependence on x which is caused by the low T_C of Fe_3Pt phase with $x=75-79$. The big difference in T_C between the heating and cooling thermomagnetic curves of the Fe–Pt alloys with $x=79-90$ can be attributed to the difference of $\alpha \Leftrightarrow \gamma$ phase transition temperature during heating and cooling. On the other hand, T_C of the $L1_0$ FePt nanoparticles was found to be strongly size dependent.
 [DOI: 10.1063/1.2709739]

I. INTRODUCTION

The interesting magnetic properties of the bulk Fe_xPt_{100-x} materials have been studied in the whole compositional region. For $x=25$ antiferromagnetic order was found;[1,2] around $x=50$ the alloy shows very large magnetic anisotropy owing to the formation of chemically ordered face-centered-tetragonal (fct) structure.[3,4] Near $x=75$ large volume instability (Invar effect) is observed in the $L1_2$ Fe_3Pt phase (γ_1).[5,6] The most recent interests in FePt nanostructured materials have been focused on the ferromagnetic $L1_0$ FePt phase (γ_2) because of their potential applications in ultrahigh-density magnetic recording[7,8] and advanced permanent magnets[9,10] due to its very high uniaxial magnetocrystalline anisotropy and high Curie temperatures. Recently, it was reported that Curie temperature (T_C) of sputtered FePt films is composition dependent in the range of 47.5–54.4 at. % Fe.[11–13] More interestingly, reduction of T_C with decreasing dimension of the materials has also been observed in $L1_0$ FePt nanoparticles[14] and other ferromagnets.[15,16] In order to understand magnetic ordering of the nanostructured ferromagnetic phases in a wide compositional range, the annealed FePt nanocrystalline films deposited by nanoparticles have been studied with a composition range of 15–90 at. % Fe. The size dependence of T_C of $L1_0$ FePt nanoparticles has also been studied.

II. EXPERIMENTS

The disordered face-centered-cubic (fcc) Fe_xPt_{100-x} nanoparticles were chemically synthesized by the standard airless chemical solution procedures.[7,17] The composition was controlled by adjusting the molar ratio of iron pentacarbonyl $Fe(CO)_5$ to platinum acetylacetonate $Pt(acac)_2$. The synthesized nanoparticles were then deposited on a Si substrate and annealed under forming gas ($Ar+7\%H_2$) at 973 K for 1 h to transfer the disordered fcc structure to the ordered $L1_0$ or $L1_2$ structure. The composition of the synthesized FePt nanoparticles was checked by energy dispersive x-ray (EDX) analysis. The crystalline structure was determined by x-ray diffraction (XRD). The room-temperature magnetic properties were studied by a superconducting quantum interference device (SQUID) magnetometer with a maximum applied field of 7 T. Thermomagnetic curves were measured by a physical property measurement system (PPMS) with high-temperature vibrating sample magnetometer.

III. RESULTS AND DISCUSSIONS

Figure 1 gives the composition dependence of the 4 nm synthesized Fe_xPt_{100-x} nanoparticles on the molar ratio of $Fe(CO)_5$ to $Pt(acac)_2$. The error bar is based on the statistical standard deviation of the EDX analysis. It shows that the composition $x=15-90$ can be obtained by adjusting the molar ratio of precursors. This result is similar to that of Ref. 17.

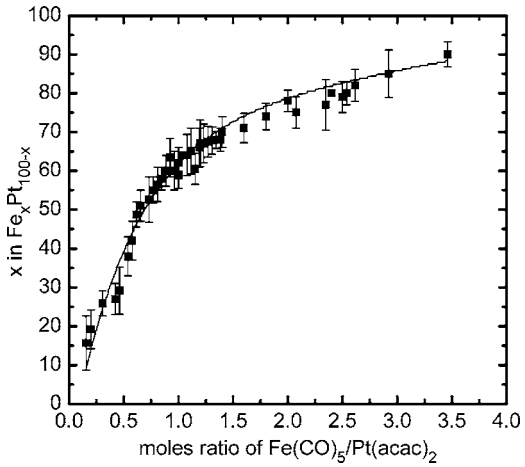

FIG. 1. The dependence of x on the molar ratio of $Fe(CO)_5$ to $Pt(acac)_2$.

[a)]Electronic mail: pliu@uta.edu

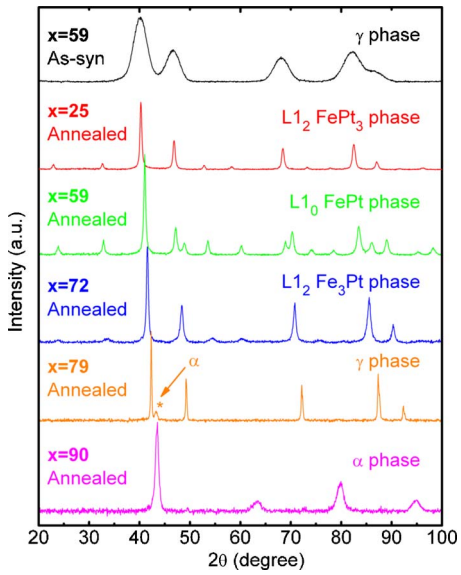

FIG. 2. (Color online) XRD patterns of the as-synthesized nanoparticles with $x=59$ and the annealed films with different compositions, i.e., $x=25$, 59, 72, 79, and 90.

XRD patterns of Fe_xPt_{100-x} films were recorded after being annealed at 973 K in forming gas for 1 h. Figure 2 shows the XRD patterns of the annealed films with five different compositions $x=25$, 59, 72, 79, and 90. A typical XRD pattern for the as-synthesized nanoparticles is also shown in the figure for comparison. It should be noted that XRD spectra of all the as-synthesized samples showed a disordered γ phase in the whole compositional region. When the assembled films were annealed at 973 K, on the other hand, $Fe_{25}Pt_{75}$ exhibits a Cu_3Au-type γ_3-$FePt_3$ phase with $L1_2$ structure. It was found that for the annealed $Fe_{59}Pt_{41}$ film the superlattice reflections (001) and (110) appear in the XRD spectra, indicating the formation of an ordered $L1_0$ γ_2-FePt phase. For $Fe_{72}Pt_{28}$, the annealing resulted in the formation of $L1_2$ γ_1-Fe_3Pt phase. With increasing Fe content to $x=79$, XRD pattern revealed that the main phase was γ-FePt phase with fcc structure, while a small amount of α-(Fe,Pt) was also found. Further increase of Fe content led to a decrease of γ-FePt phase content and an increase of α-FePt phase content. When $x=90$, the annealed films consisted of only α-FePt phase, as shown in Fig. 1. In general, the peak broadening of the annealed Fe_xPt_{100-x} films became less pronounced compared to the as-synthesized nanoparticles since the grains became coarse upon annealing. The average grain size was 4 nm for the as-synthesized nanoparticles, while it was around 10–20 nm after annealing on Si substrates, determined by the analysis of XRD patterns using Scherrer formula.

Figure 3 shows the dependence of Néel temperature T_N or Curie temperature T_C on composition of the annealed nanoparticles. The magnetic phase transition temperatures were determined by the intersection of extrapolations of the greatest slope and flat region in the M-T curves. It was reported that $FePt_3$ is antiferromagnetic in the chemically ordered state.[1,2] The XRD patterns show that the ordered phase $FePt_3$ with Cu_3Au cubic $L1_2$ structure can be obtained when $x\leqslant 40$, which is similar to the condition shown in the phase

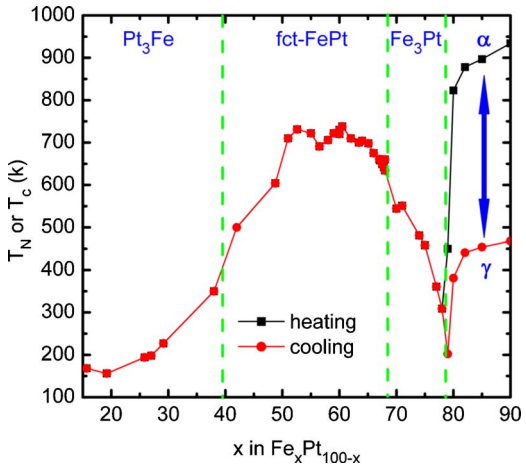

FIG. 3. (Color online) The dependence of T_N or T_C on x of the annealed nanoparticles.

diagram.[18] It was found that T_N of the $FePt_3$ phase increased with increasing Fe content. An ordered fct FePt ferromagnetic phase with $L1_0$ structure formed within the compositional region $x=40-69$. T_C of the fct phase increased fast when $x\leqslant 50$ and reached the maximum about 730 K when $x=51-64$ and then dropped with increasing x. For $69\leqslant x\leqslant 78$, Fe_3Pt phase with $L1_2$ structure was formed after annealing. It can be seen that T_C decreased dramatically from 550 K with $x=70$ to 310 K with $x=79$. More interestingly, it was found that there is a big difference between the heating and cooling thermomagnetic curves of the Fe–Pt alloys with Fe content of 80–90 at. %. Figure 4 shows the typically heating and cooling M-T curves of the $Fe_{80}Pt_{20}$ sample. This phenomenon can be attributed to the difference of $\alpha\Leftrightarrow\gamma$ phase transition temperature during heating and cooling.[19] One can see from the Fe–Pt phase diagram[18] that the phase transitional temperature from α to γ phase on heating is far higher than that of γ to α on cooling.

Figure 5 gives the dependence of saturation magnetization M_s and coercivity H_c on the composition of annealed nanoparticles. M_s at room temperature, which was measured under 7 T, increases monotonously almost in the whole compositional region except in the region $75<x\leqslant 79$ where M_s of the Fe_3Pt phase drops. This is caused by the low Curie

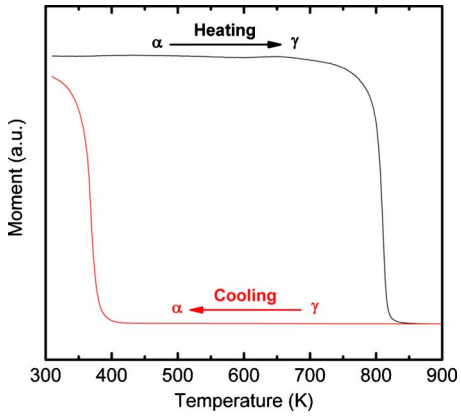

FIG. 4. (Color online) The typically heating and cooling M-T curves of the $Fe_{80}Pt_{20}$ sample.

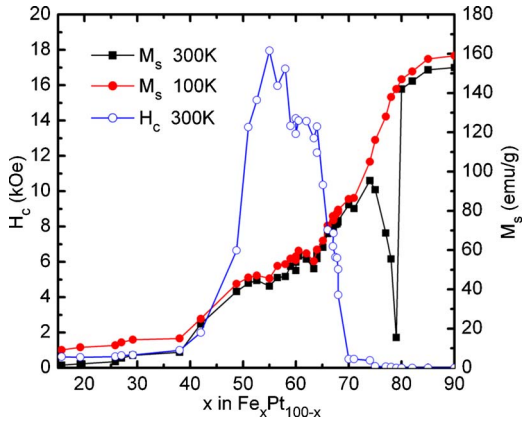

FIG. 5. (Color online) The dependence of M_s and H_c on x of annealed nanoparticles.

temperature (near or lower than room temperature) of Fe_3Pt phase in this special compositional region since there is no dip in the M_s-x curve at 100 K, as shown in Fig. 5. H_c is also very sensitive to composition. Nonzero coercivity can be obtained only in the region $x=42-68$ where $L1_0$ phase was formed. The maximum H_c is 18 kOe at $x=55$. With both high M_s and H_c, the maximum energy product $(BH)_{max}$ about 17 MG Oe can be obtained at $x=66$ where $H_c=7.6$ kOe.

Beside the composition dependence, it was also found that T_C decreases fast with decreasing dimensions of the materials. Our recently developed salt-matrix annealing method[20] allows us to tune the size of the monodisperse $L1_0$ FePt particles and to obtain a direct correlation between particle size and Curie temperature. Figure 6 shows M-T curves of the 3 and 15 nm $L1_0$ FePt nanoparticles which are obtained by the salt-matrix. It shows that T_C of the 3 nm particles is substantially lower than that of 15 nm particles. A systematic study of the size dependence of T_C has been reported elsewhere.[14] The size dependent behavior, as discussed in Refs. 14–16, can be explained by the finite-size-scaling theory.[21,22]

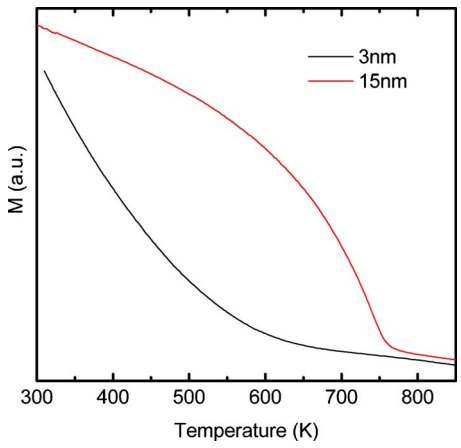

FIG. 6. (Color online) M-T curves of the 3 and 15 nm $L1_0$ nanoparticles which are obtained by the salt-matrix method.

IV. CONCLUSION

The FePt nanoparticles with controlled composition have been prepared by chemical synthesis. The ordered phases with different structures were obtained by annealing the particles at 973 K for 1 h. It is found that the $L1_0$ FePt structure can be formed in a wide compositional region of $x=40-68$, while the $FePt_3$ or Fe_3Pt with $L1_2$ structure are formed with lower or higher Fe contents. The Curie temperatures of the $L1_0$ FePt phase are strongly composition dependent and are higher than that of Fe_3Pt phase. The abnormal dependence of M_s at room temperature on x is caused by the low T_C of Fe_3Pt phase with $x=75-79$. It was also found that there is a big difference in T_C when measured through the heating and cooling thermomagnetic curves of the Fe–Pt alloys with $x=78-90$. This phenomenon can be attributed to the difference of $\alpha \Leftrightarrow \gamma$ phase transition temperature during heating and cooling. On the other hand, T_C of the $L1_0$ FePt nanoparticles is strongly size dependent.

ACKNOWLEDGMENTS

This work was supported by US DoD/MURI Grant No. N00014-05-1-0497 and DARPA through ARO under Grant No. DAAD 19-03-1-0038.

[1] G. E. Bacon and J. Crangle, Proc. R. Soc. London, Ser. A **272**, 387 (1963).
[2] S. Maat, O. Hellwig, G. Zeltzer, E. E. Fullerton, G. J. Mankey, M. L. Crow, and J. L. Robertson, Phys. Rev. B **63**, 134426 (2001).
[3] H. Kanazawa, G. Lauhoff, and T. Suzuki, J. Appl. Phys. **87**, 6143 (2000).
[4] S. Okamoto, N. Kikuchi, O. Kitakami, T. Miyazaki, Y. Shimada, and K. Fukamichi, Phys. Rev. B **66**, 024413 (2002).
[5] R. Hayn and V. Drchal, Phys. Rev. B **58**, 4341 (1998).
[6] M. Matsushita, Y. Miyoshi, S. Endo, and F. Ono, Phys. Rev. B **72**, 214404 (2005).
[7] S. H. Sun, C. B. Murray, D. Weller, L. Folks, and A. Moser, Science **287**, 1989 (2000).
[8] C. Ross, Annu. Rev. Mater. Res. **31**, 203 (2001).
[9] H. Zeng, J. Li, J. P. Liu, Z. L. Wang, and S. H. Sun, Nature (London) **420**, 395 (2002).
[10] C. B. Rong, H. W. Zhang, X. B. Du, J. Zhang, S. Y. Zhang, and B. G. Shen, J. Appl. Phys. **96**, 3921 (2004).
[11] K. Barmak, J. Kim, S. Shell, E. B. Svedberg, and J. K. Howard, Appl. Phys. Lett. **80**, 4268 (2002).
[12] K. Barmak, J. Kim, D. C. Berry, K. Wierman, E. Svedberg, and J. K. Howard, J. Appl. Phys. **95**, 7486 (2004).
[13] K. Barmak, J. Kim, D. C. Berry, W. N. Hanani, K. Wierman, E. B. Svedberg, and J. K. Howard, J. Appl. Phys. **97**, 024902 (2005).
[14] C. B. Rong, D. R. Li, V. Nandwana, N. Poudyal, Y. Ding, Z. L. Wang, H. Zeng, and J. P. Liu, Adv. Mater. (Weinheim, Ger.) **18**, 2984 (2006).
[15] M. Farle, K. Baberschke, U. Stetter, A. Aspelmeier, and F. Gerhardter, Phys. Rev. B **47**, 11571 (1993).
[16] J. P. Chen, C. M. Sorensen, K. J. Klabunde, and G. C. Hadjipanayis, Phys. Rev. B **54**, 9288 (1996).
[17] S. H. Sun, E. E. Fullerton, D. Weller, and C. B. Murray, IEEE Trans. Magn. **37**, 1239 (2001).
[18] M. Hausen and K. Anderko, *Constitution of Binary Alloys* (McGraw-Hill, New York, 1958).
[19] J. Martelly, Ann. Phys. (N. Y.) **9**, 318 (1938).
[20] K. Elkins, D. Li, N. Poudyal, V. Nandwana, Z. Q. Jin, K. H. Chen, and J. P. Liu, J. Phys. D **38**, 2306 (2005).
[21] K. Binder, Physica (Amsterdam) **62**, 508 (1972).
[22] S. N. Kaul, J. Magn. Magn. Mater. **53**, 5 (1985).